Hadronic collisions: physics, models and event generators used for simulating the cosmic ray cascade at the highest energies

J. Ranft[1]

Physics Dept. Universität Siegen, D–57068 Siegen, Germany, e–mail: Johannes.Ranft@cern.ch

Siegen preprint SI–01–01

Extended version of a paper to be published in the proceedings of the meeting Monte Carlo 2000, Lisboa, Oct. 2000

1 Introduction

Models and event generators for hadronic collisions belong to the basic building blocks of hadron cascade calculations to simulate radiation problems around high energy accelerators and to simulate the Cosmic Ray cascade in the atmosphere, within the earth or within space stations. At the same time these models often have to describe also the new physics to be investigated at a given accelerator, examples are the present study of photon–photon collisions at the LEP collider or the study of central collisions of heavy ions at the CERN–SPS and at the RHIC and LHC colliders.

There are at least two main applications of such models to study radiation problems around accelerators and colliders:

(i)At colliders like the LHC one of the main radiation sources are the proton–proton or nucleus–nucleus collisions inside the detectors. Present and future colliders are also to investigate $e^+ - e^-$, $\mu^+ - \mu^-$ and photon–photon collisions. Therefore, also models for hadronic collisions of leptons and photons become more and more important for the study of radiation problems.

(ii)The second application is for the transport of the produced particles in the elements of the detectors and accelerators and in the shielding material. For this we have to understand hadron–nucleus, nucleus–nucleus, lepton–nucleus, photon–nucleus and even neutrino–nucleus collisions at all energies.

Here we are concerned with hadronic models or event generators for hadronic collisions. These models are inserted into hadron cascade codes to study the radiation transport. We will not discuss hadron cascade codes here, but some of them are mentioned when discussing the application of the hadronic models. There are also cases, where a dedicated hadronic model is formulated within the hadron cascade code.

The models for hadronic collisions have to provide the produced hadrons preferably in the form of Monte Carlo events as well as the inelastic cross sections of the collisions considered. The event generators of interest for our applications have to provide minimum bias events, not only events for selected (hard) collisions, which might be the main object of the physics studied at a given collider. We need detailed models for all collisions, not only for interesting events, where for instance SUSY particles or Higgs bosons might be produced. In recent years new features of hadronic collisions have been found experimentally which were not predicted by any of the models. Therefore, the models have to be continuously updated and revised in order to reproduce all known properties of the collisions. Some of these features are: (i)Hard diffraction [1,2] and events with large rapidity gaps between jets [3,4]. (ii)Enhanced stopping of leading baryons in nuclear collisions [5,6], one way to incorporate this into the multi–string models is by considering new string configurations (diquark–breaking diagrams) [7,8].

2 Models for hadronic interactions

Unfortunately, it is not possible to discuss here all existing Monte Carlo models for hadron production. Let me at least mention some important models, which I will not discuss:

(i)There are JETSET [9], PYTHIA [10], HERWIG [11] and ISAJET [12], which are mainly used to sample selected classes of events. These are certainly the event generators used most extensively by collider experiments. Codes not discussed, mainly for reasons of space, are also HIJING [13] and FRITIOF [14], both are codes for nuclear collisions.

(ii)There are dedicated event generators inside hadronic codes like FLUKA, HERMES, MARS, MCNPX, NMTC or GEANT. Usually these are not available as separate codes. The event generators inside all of these codes will be covered by contributions to this Meeting (examples: FLUKA: [15] GEANT: [16]). Therefore, there is no need for me to discuss them.

(iii)PHOJET [17,18] is a minimum bias Dual Parton Model event generator with a very broad applicability for hadrons, photons and electrons as projectiles and targets. PHOJET is contained in the new DPMJET–III event generator, which adds nuclei as targets and projectiles to the above PHOJET list. DPMJET–III will for the first time be described at this meeting [19].

In this talk I will only discuss hadronic models which work above a mimimum lab–energy of about 5 GeV per nucleon and with a maximum lab–energy of about 10^{11} GeV or (in the units used in Cosmic Ray applications 10^{21} eV), this means codes which are also available for studying the Cosmic Ray cascade up to the highest energy.

The extension of models for multiparticle production in hadron–hadron, hadron–nucleus and nucleus–nucleus collisions to be used for the simulation of the Cosmic Ray cascade up to $E_{lab} = 10^{21}$ eV (corresponding for p–p collisions to $\sqrt{s} = 2000$ TeV) is needed to prepare for the Auger experiment [20] as well as for a reliable interpretation of present experiments like AGASA [21], Fly's Eye [22] and High Resolution Fly's Eye [23,24] , which present data in the EeV energy region.

Nearly all event generators for hadronic or nuclear collisions in the considered energy range are constructed out of the following ingredients:

(i)In hadron–hadron collisions or in elementary nucleon–nucleon collisions of nuclear collisions multiple soft color singlet chains with quarks, diquarks and antiquarks at their ends are formed according to the rules of Gribov–Regge theory together with topological arguments. This are mainly diquark–quark and quark–antiquark chains. The Gribov–Regge theory also gives all the hadron–hadron cross sections.

(ii) In collisions involving nuclei one starts with the construction of multiple interactions according to the Gribov–Glauber theory. In simple models each collision leads just to the formation of one pair of colorless chains. In evolved models there is the full multi–chain system according to (i) and (iii) in each elementary collision. The Gribov–Glauber theory gives not only the distribution in the numbers of elementary collisions, it gives also the nuclear cross–sections in terms of the elementary (input) nucleon–nucleon cross–sections. There are also simplified models, which do not treat the full Gribov–Glauber theory for nucleus–nucleus collisions. In these models (using the superposition model) the nucleus–nucleus collision is replaced by a couple of hadron–nucleus collisions.

(iii) At sufficiently large energy besides the soft chains according to (i) and (ii) we have a system of multiple minijets. At high collision energies hard and semihard parton–parton collisions occur and become more and more important with rising collision energy. The produced jets and minijets become important features of most models, they determine the transverse momentum or transverse energy properties of the models at high energy. The input cross section for semihard multiparticle production (or minijet production) σ_h is calculated applying the QCD improved parton model, the details are given (for instance as implemented in DPMJET) in Ref.[25,26,27,28].

$$\sigma_h = \sum_{i,j,k,l} \int_0^1 dx_1 \int_0^1 dx_2 \int d\hat{t} \; \frac{1}{1+\delta_{kl}} \frac{d\sigma_{QCD,ij\to kl}}{d\hat{t}} \\ \times f_i(x_1,Q^2) f_j(x_2,Q^2) \; \Theta(p_\perp - p_{\perp thr}) \qquad (1)$$

$f_i(x,Q^2)$ are the structure functions of partons with the flavor i and scale Q^2 and the sum i,j,k,l runs over all possible flavors. Now after the HERA measurements of structure functions at small Bjorken x_{bj} it is very essential to use modern structure functions, which agree to the HERA data. Since the HERA measurements, the structure functions are known to behave at small x like $1/x^\alpha$ with α between 1.35 and 1.5. To remain in the region where perturbation theory is valid, a low $p_\perp$ cut–off, $p_{\perp_{thr}}$, is used for the minijet component. The multiplicity distribution for the minijets is obtained by an unitarization procedure.

(iv)After forming all partonic chains according to (i) to (iii) the next step is initial state and final state QCD evolution of all hard chains, after this all chains are hadronized using the Lund codes JETSET or PYTHIA or in some codes private dedicated codes for string hadronization.

(v)There are special cases of hadron production in hadron–hadron, hadron–nucleus and nucleus–nucleus collisions, these are diffractive interactions (or interactions with rapidity gaps between the produced particles). Diffractive hadron production is usually treated in special routines. Since the discovery of hard processes also in diffractive interactions at the CERN-SPS collider, HERA and at the TEVATRON (for instance jet–gap–jet events) this has become more complicated than before, only very few codes (for instance PHOJET and with this DPMJET–III) include at present hard diffraction. However, there exist dedicated codes for the simulation of hard diffraction.

(vi) After steps (i) to (v) we have events consisting out of produced hadrons (from string fragmentation) and spectators (these are nucleons from the original projectile and target nuclei, which have not taken part in the interaction). In the next step the codes treat secondary interactions. This is in simple cases just a formation zone intranuclear cascade, where the produced hadrons interact with the spectators, a more complete treatment is the full secondary hadron cascade, where the produced hadrons interact with the spectators as well as with other produced co–moving hadrons. There are also codes, where the secondary interactions occur already at the level of the chains before hadronization or at the level of chain–end partons before the formation of the color neutral chains.

(vii)Now we have the produced hadrons and the remains of the projectile and target nucleus (in the form of spectator nucleons with no interactions or only interactions which were not able to knock them out of the nuclear potential). These remains are considered as excited residual nuclei, which in a following evaporation step deexcite by the emission of evaporation particles (protons, neutrons and nuclear fragments). Finally the excited nuclei, which no longer are able to emit evaporation particles emit deexcitation photons to form finally a stable (or radioactive) residual nucleus.

Let us summarize important aspects of some event generators used often in calculating the Cosmic Ray cascade:

The DPMJET–II.5 event generator based on the two–component Dual Parton Model (DPM) was described in detail [29,30,31,32,33,7]. DPMJET–II.5 describes well minimum bias hadron and hadron jet production up to present collider energies. DPMJET is used for the simulation of the Cosmic Ray cascade within the HEMAS–DPM code [34] used mainly for the MACRO experiment [35]. DPMJET–II.5 will soon be available within the CORSIKA cosmic ray cascade code[36].

The SIBYLL–1.7 model [37] is a minijet model and has been reported to be applicable up to $E_{lab} = 10^{20}$ eV. However, the EHLQ [38] parton structure functions used for the calculation of the minijet component might , after the HERA experiments, no longer be adequate. It is known, that a significant updating of SIBYLL is on the way [39], but the new code is not yet available. SIBYLL is a popular model for simulating the Cosmic Ray cascade in the USA. SIBYLL is available within the CORSIKA cosmic ray cascade code[36] and within the AIRES [40] and MOCCA [41,42] cosmic ray cascade codes .

VENUS [43], a popular model applied originally mainly for describing heavy ion experiments. VENUS is applicable up to $E_{lab} = 5{\times}10^{16}$ eV. It has been reported [44], that the introduction of minijets into VENUS has been planned, this will allow to apply VENUS up to higher energies. A new version of VENUS called *neXus*[45] was not yet to be available for distribution at the time, when my talk was prepared, it will be available in the next release of the CORSIKA cosmic ray cascade code.

QGSJET [46] is the most popular Russian event generator used for Cosmic Ray simulations. It is based on the Quark Gluon String (QGS) model, this model is largely equivalent to the DPM. QGSJET also contains a minijet component and is reported to be applicable up to $E_{lab} = 10^{20}$ eV. QGSJET is available within the CORSIKA cosmic ray cascade code[36] and within the AIRES [40] cosmic ray cascade code.

In Table 1 we present some characteristics of the models. The Gribov–Regge theory is applied by three of the models. The pomeron intercept for SIBYLL is equal to one, SIBYLL is a minijet model using a critical pomeron, with only one soft chain pair, all the rise of the cross section results from the minijets. In the models with pomeron intercept bigger than one, we have also multiple soft chain pairs, already the soft pomeron leads to some rise of the cross sections with energy. Minijets are used in three of the models, it is believed, that minijets are necessary to reach the highest energies. All models contain diffractive events. Secondary interactions between all produced hadrons and spectators exist only in VENUS, DPMJET has only a formation zone intranuclear cascade (FZIC) between the produced hadrons and the spectators. Only three of the models sample properly nucleus–nucleus collisions, SIBYLL replaces this by the semi–superposition model [47]. The residual projectile (and target) nuclei are only given by two of the models.

Table 1. Characteristics of some popular models for hadron production in Cosmic Ray cascades.

	VENUS	QGSJET	SIBYLL	DPMJET
Gribov–Glauber	x	x	x	x
Gribov–Regge	x	x		x
Pomeron intercept	1.07	1.07	1.00	1.05
minijets		x	x	x
diffractive events	x	x	x	x
secondary interactions	x			x
A–A interactions	x	x		x
superperposition model			x	
nuclear evaporation, residual nuclei		x		x
maximum Energy [GeV]	10^7	10^{11}	10^{11}	10^{12}

Each model has to determine its free parameters. This can be done by a global fit to all available data of total, elastic, inelastic, and single diffractive cross sections in the energy range from ISR to collider experiments as well as to the data on the elastic slopes in this energy range. Since there are some differences in the hard parton distribution functions at small x values resulting in different hard input cross sections we have to perform separate fits for each set of parton distribution functions. After this stage each model predicts the cross sections also outside the energy range, where data are available.

3 Code comparisons

There is certainly the need to understand the systematic errors of the hadronic models and event generators. (i) This is more easy in all the region, where experimental data exist. Here it is useful to compare the models to as many experimental data as possible. It is a task of the community to decide about the most suitable benchmark experiments. We can however assume, that most published models agree to most of the available data.

Systematic errors of models are more difficult to estimate in regions, where no experimental data are available. This might be collisions at energies beyond the energies of existing accelerators or in regions of the phase space, where no experimental data are available. A very prominent example for the latter is the fragmentation region at large Feynman–x, which was never studied in hadron production experiments at the highest energies available at the CERN–SPS collider and at the TEVATRON collider, but just this fragmentation region is of upmost importance for the Cosmic Ray cascade. The systematic comparison of Monte Carlo models in such regions is very useful to understand how reliable the extrapolations of the models into such regions might be.

The Karlsruhe code comparison [48] was a first extensive comparison of Monte Carlo models, which are available as event generators within the CORSIKA Cosmic Ray cascade code [36,49]. The energies, mainly in the 10^{14} and 10^{15} eV range and the distributions chosen in this comparison were motivated by the interest of the KASKADE[50] experiment in Karlsruhe. With one exception, I will not review this code comparison here. A code comparison extending up to higher energies was performed within the AIRES [40] code system [51].

Further code comparisons should be strongly encouraged. Some extensions to higher energy of such a code comparison were presented in talks by Engel [52,53].

Here I will present some code comparisons up to the highest energies, for which the models are able to run. The first idea was just to use the event generators implemented in the last distributed version CORSIKA–5.61 [49]. But there was only the older version DPMJET–II.4 implemented. So I use for DPMJET my stand–alone version of DPMJET–II.5 [32,33,7]. With SIBYLL–1.6 as implemented in CORSIKA–5.61 I got funny results at high energy (above 10^{18} eV) (I understand, that these problems with SIBYLL–1.6 are now corrected in CORSIKA.). Using the stand–alone code SIBYLL–1.7, the last SIBYLL version distributed by the authors, these anomalies disappeared, therefore I use for SIBYLL only the stand–alone version mentioned. With QGSJET in CORSIKA, I did not find any problems, so I use it in the form as implemented in CORSIKA–5.61. The VENUS code as implemented in CORSIKA–5.61 runs only up to 10^{16} eV. With this it is not possible to go beyond the Karlsruhe code comparison [48].

In all the following plots I present and compare the result of the three event generators in the implementations as mentioned. The first comparisons are for p–N (proton–Nitrogen) collisions, p–N collisions are a good approximation to p–Air collisions which are important for the Cosmic Ray cascade.

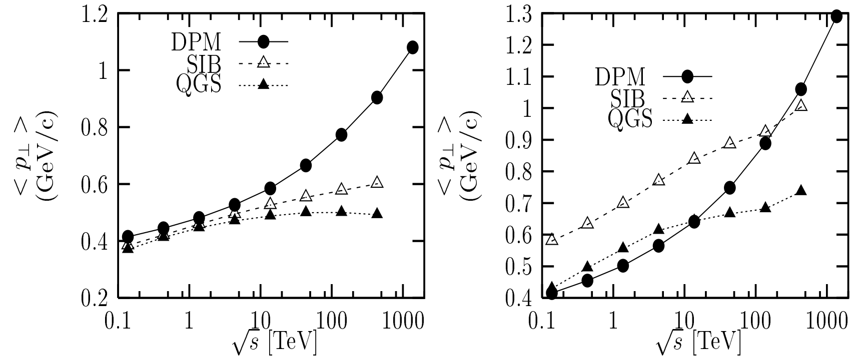

Fig. 1. **(a)** Average transverse momenta for charged hadron production in p–N (proton–Nitrogen) collisions as function of the (nucleon–nucleon) cms energy $\sqrt{s}$. **(b)** Average transverse momenta for proton production in p–N (proton–Nitrogen) collisions as function of the (nucleon–nucleon) cms energy $\sqrt{s}$.

In Fig.1.a we present average transverse momenta of charged hadrons as obtained from DPMJET–II.5, QGSJET and SIBYLL for p–N collisions as function of the cms energy $\sqrt{s}$. At energies where data (in p–p or p–$\bar{p}$ collisions) exist all models agree rather well with each other and with the data. However, we find completely different extrapolations to higher energies. We should note, all three models have a minijet component. But it seems, that in spite of the minijets the average transverse momentum in QGSJET becomes constant at high energies, while it continues to rise in DPMJET. We can conclude, there are very big differences in implementing the minijet components in the models. There are even bigger differences in the models, if we consider the average transverse momenta of secondary protons, see Fig.1.b. DPMJET and QGSJET diverge like in Fig.1.a and the prediction of SIBYLL–1.7 is even at lower energies, where we find agreement between all three models in Fig.1.a, significantly outside the other models.

Fig.2.a presents the rise of the total charged multiplicity and Fig.2.b presents the rise of the secondary proton multiplicity with the cms energy $\sqrt{s}$ according to DPMJET, QGSJET and SIBYLL. We find again, at low energies, where data are

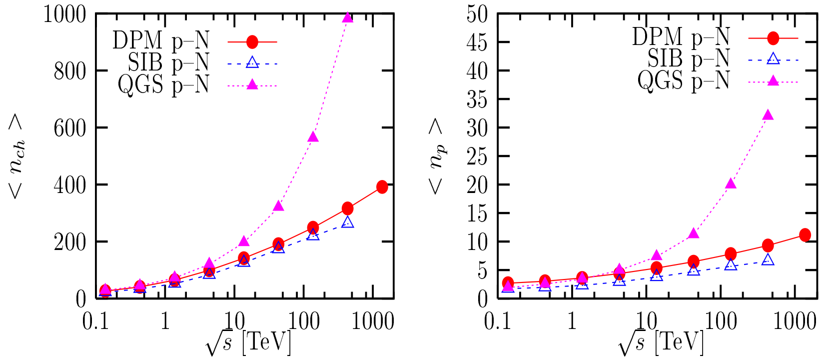

Fig. 2. (a) The average multiplicity of charged hadron production in p–N (proton–Nitrogen) collisions as function of the (nucleon–nucleon) cms energy $\sqrt{s}$. **(b)** The average multiplicity of secondary proton production in p–N (proton–Nitrogen) collisions as function of the (nucleon–nucleon) cms energy $\sqrt{s}$.

available, the models agree rather well. DPMJET and SIBYLL agree in all the energy range shown. However, QGSJET above the energy of the TEVATRON extrapolates to higher energies in a completely different way.

In Fig.3.a and 3.b we present for p–N collisions the energy fractions K of charged pion production and for net–baryon $B - \bar{B}$ production (Since newly produced baryons and anti–baryons are expected to carry the same energy fractions, this corresponds to the energy carried by the baryons which were present before the collision, which have been stopped and transformed by the collision.). In the case of $K_{B-\bar{B}}$ we find all three models to behave widely different, in the case of K_{π^+,π^-} we find DPMJET and QGSJET to agree largely, but SIBYLL behaves quite differently. Here I should mention, that new baryon stopping diagrams [54,55] have so far only been implemented in DPMJET–II.5. This enhanced stopping is responsible for $K_{B-\bar{B}}$ being smaller and K_{π^+,π^-} being bigger in DPMJET–II.5 than in the other two models.

The cosmic ray spectrum–weighted moments [56] in p–A collisions are defined as moments of the $F(x_{lab}) = x_{lab} dN/dx_{lab}$:

$$f_i^{p-A} = \int_0^1 (x_{lab})^{\gamma-1} F_i^{p-A}(x_{lab}) dx_{lab} \tag{2}$$

Here $-\gamma \simeq -1.7$ is the power of the integral cosmic ray energy spectrum and A represents both the target nucleus name and its mass number.

In Fig.4.a and 4.b we present the spectrum weighted moments for pion and Kaon production in p–N collisions as function of the cms energy $\sqrt{s}$ per nucleon. In contrast to Fig. 3 we find this time DPMJET and SIBYLL to agree approximately, but QGSJET behaves completely different.

In Figs. 5.a and 5.b we present the extrapolations to high energy E_{lab} of the x_{lab} distributions dN/dx_{lab} for secondary protons produced according to the models DPMJET–II.5 and QGSJET. The distributions are plotted for E_{lab} =

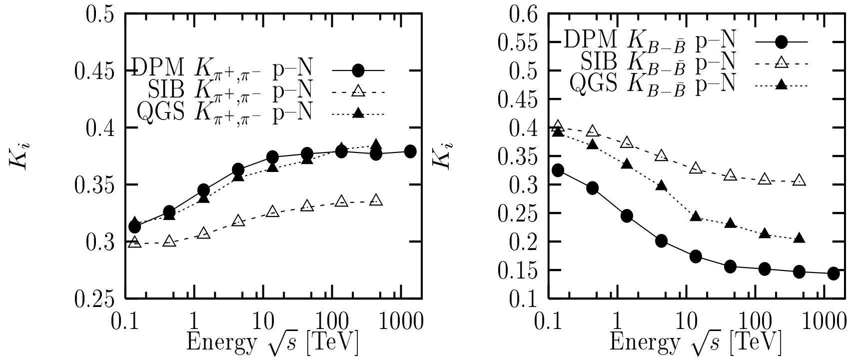

Fig. 3. **(a)** Average energy fraction for charged pion π^+, π^- production K_{π^+,π^-} in p–N collisions as function of the (nucleon–nucleon) cms energy $\sqrt{s}$. **(b)** Average energy fraction for net baryon $B - \bar{B}$ production $K_{B-\bar{B}}$ in p–N collisions as function of the (nucleon–nucleon) cms energy $\sqrt{s}$.

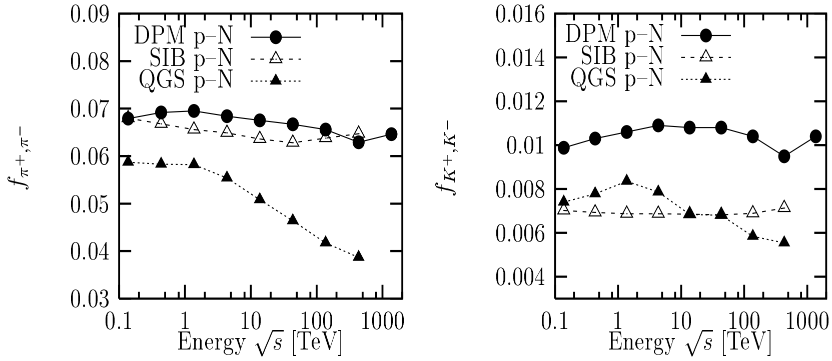

Fig. 4. **(a)** Spectrum weighted moments for charged pion production f_{π^+,π^-} in p–N collisions as function of the (nucleon–nucleon) cms energy $\sqrt{s}$. **(b)** Spectrum weighted moments for charged Kaon production f_{K^+,K^-} in p–N collisions as function of the (nucleon–nucleon) cms energy $\sqrt{s}$.

10^{13}, 10^{16} and 10^{20} eV . At the lowest energy the two models agree roughly, but there are considerable differences in the extrapolations to 10^{16} and 10^{20} eV. The differences between DPMJET–II.5 and SIBYLL–1.7 are mainly due to the baryon stopping diagrams implemented in DPMJET–II.5 [7,8] but not present in SIBYLL–1.7. The scaling behavior of the distributions according to DPMJET–II.5 and SIBYLL–1.7 is nearly perfect in the x_{lab} region from 0.1 to 0.6, but this is just the region where the non–scaling appears in QGSJET. The behavior of the models in p–p and p–$\bar{p}$ is rather similar to the one in p-N collisions. Clearly, measurements of leading baryon distributions at the TEVATRON and at the LHC will resolve the conflict between the three models.

Similarly, in Figs. 6.a and 6.b we present the extrapolations to high energy E_{lab} of the x_F distributions $F(x_F)$ for secondary π^+ produced according to the models DPMJET–II.5 and QGSJET. The distributions are again plotted for E_{lab} = 10^{13}, 10^{16} and 10^{20} eV . SIBYLL–1.7 behaves similar to DPMJET–II.5 but as seen before DPMJET–II.5 and QGSJET differ considerably in the shape of the distributions, only measurements at the highest possible energies can resolve the situation.

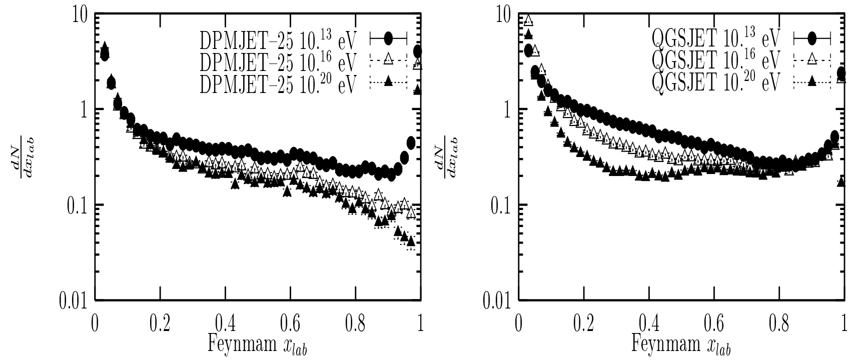

Fig. 5. **(a)** x_{lab}–distributions of secondary protons produced in p–N collisions at E_{lab} = 10^{13}, 10^{16} and 10^{20} eV according to the DPMJET–II.5 model. **(b)**x_{lab}–distributions of secondary protons produced in p–N collisions at $E_{lab} = 10^{13}$, 10^{16} and 10^{20} eV according to the QGSJET model.

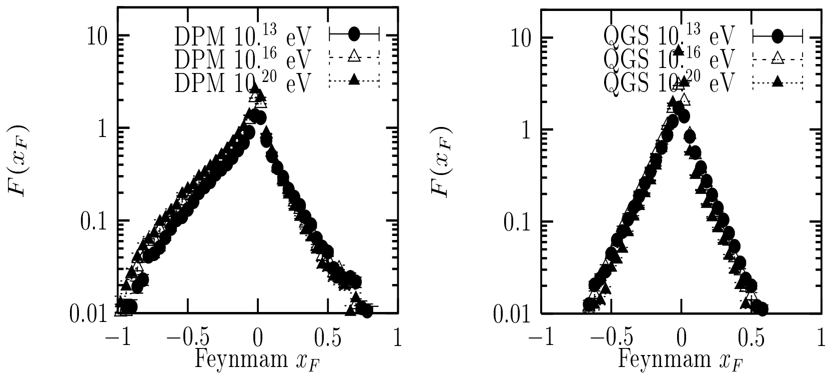

Fig. 6. **(a)** x_F–distributions of secondary π^+ produced in p–N collisions at $E_{lab} = 10^{13}$, 10^{16} and 10^{20} eV according to the DPMJET–II.5 model. **(b)**x_F–distributions of secondary π^+ produced in p–N collisions at $E_{lab} = 10^{13}$, 10^{16} and 10^{20} eV according to the QGSJET model.

In the next four Figures we will demonstrate, that the differences in the extrapolations to high energy in Fe–N collisions are at least as large as in p–p or p–N collisions. However we find also, that in Fe–N collisions QGSJET does not run up to such high energies as DPMJET and SIBYLL.

For a better comparison with our p–N Figures, we plot also the Fe–N comparisons up to $\sqrt{s}$ = 1000 TeV per nucleon–nucleon collision. What is needed for cosmic ray simulations are lab energies up to 10^{20} to 10^{21} eV per nucleus, the energies reached with QGSJET are sufficient for this.

In Fig. 7.a we compare average $< p_\perp >$ of produced charged hadrons as function of the (nucleon–nucleon) cms energy $\sqrt{s}$ in Fe–N collisions. The differences between the three models look very similar to the differences found in p–N collisions in Fig.1.a. In Fig. 7.b we compare the multiplicity of produced charged hadrons as function of the (nucleon–nucleon) cms energy $\sqrt{s}$ in Fe–N collisions. Here the differences between the three models look completely different than in p–N collisions in Fig.2.a.

In Fig. 8,a we compare the average energy fraction for charged pion π^+, π^- production K_{π^+,π^-} in Fe–N collisions as function of the (nucleon–nucleon) cms energy $\sqrt{s}$. At low energies K_{π^+,π^-} rises with $\sqrt{s}$ for all three models and the absolute magnitudes differ by less than 20 percent. However, starting at $\sqrt{s}$ = 5 TeV for QGSJET K_{π^+,π^-} starts to decrease strongly, while for the other two models K_{π^+,π^-} continues to rise with $\sqrt{s}$.

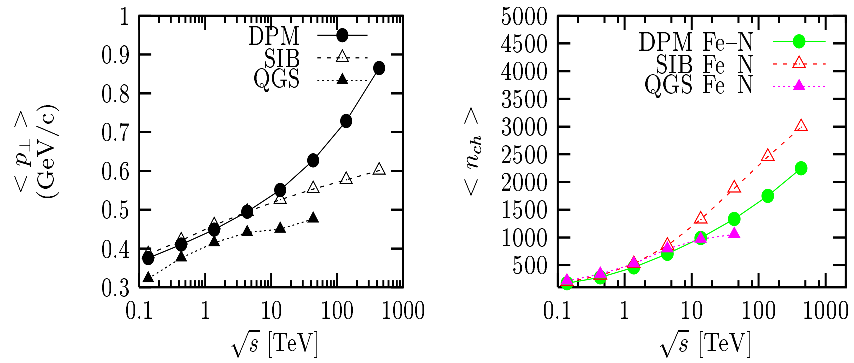

Fig. 7. (a) Average transverse momenta for charged hadron production in Fe–N collisions as function of the (nucleon–nucleon) cms energy $\sqrt{s}$. **(b)** Average multiplicity of charged hadron production in Fe–N collisions as function of the (nucleon–nucleon) cms energy $\sqrt{s}$.

In Fig. 8.b we observe a quite similar behavior of the spectrum weighted moments for charged pion production f_{π^+,π^-} in Fe–N collisions as function of the (nucleon–nucleon) cms energy $\sqrt{s}$. Now the curves for DPMJET–II.5 and SIBYLL–1.7 rise in a similar way with $\sqrt{s}$, but the absolute size differs considerably. For QGSJET we find , similarly to the last Figure a decrease starting at about $\sqrt{s}$ = 5 TeV.

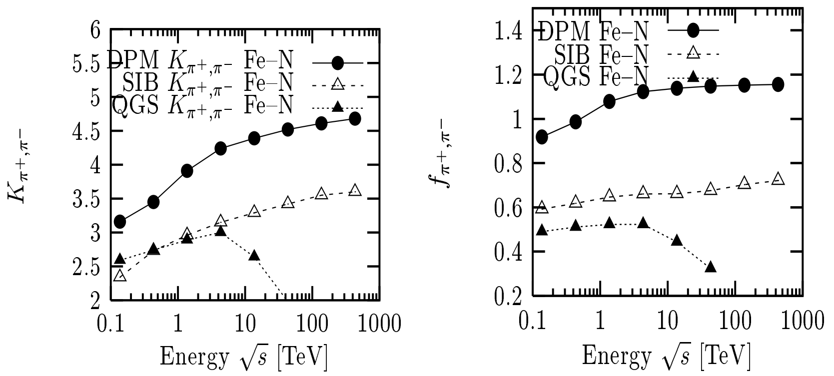

Fig. 8. **(a)** Average energy fraction for charged pion π^+, π^- production K_{π^+,π^-} in Fe–N collisions as function of the (nucleon–nucleon) cms energy $\sqrt{s}$. **(b)** Spectrum weighted moments for charged pion production f_{π^+,π^-} in Fe–N collisions as function of the (nucleon–nucleon) cms energy $\sqrt{s}$.

Comparison of the models after simulating the Cosmic Ray cascade

Next we present one comparisons from the Karlsruhe code comparison [48], which refers to the Cosmic Ray cascade simulated with different event generators.

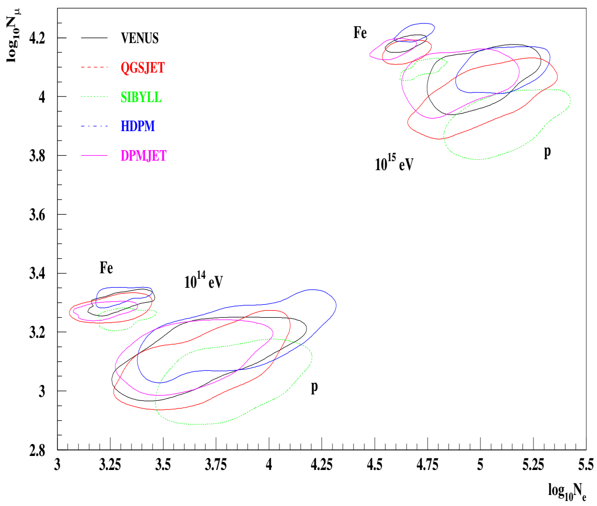

Fig. 9. Contours in the $\log_{10} N_\mu$ –$\log_{10} N_e$ plane for p and Fe induced showers of $E = 10^{14}$ and 10^{15} eV . The distributions were calculated using the CORSIKA shower code [48] with 5 different event generators for the hadronic interactions. The HPDM code[57] not mentioned before in this talk is a DPM similar model.

The distribution chosen in this comparison is motivated by the interest of the KASKADE[50] experiment in Karlsruhe.

In Fig. 9 Fe and p induced showers with energies of $E = 10^{14}$ and 10^{15} eV are plotted in the $\log_{10} N_\mu$ –$\log_{10} N_e$ plane (Muon–number –Electron–number plane). The distribution of events according to each of the 5 interaction models for each energy and primary particle is indicated by contours. Considering such a plot calculated with only one of the models, where Muon number is plotted over electron number, the impression is, that a simultaneous measurement of Muon–number and Electron number allows to determine the primary energy as well as the composition of the primary component. In such a plot we would see, that for instance VENUS and DPMJET agree very well, but the contour according to SIBYLL for Fe projectiles of $E = 10^{15}$ eV overlaps the VENUS and DPMJET contours for p projectiles at this energy. From these differences between the models one can conclude, that at present the systematic errors in the cascade calculation prevent to identify safely the composition of the primary component from such measurements.

4 Standardization of Monte Carlo hadronic production models

There were in the past and there are at present some activities to standardize some features of the Monte Carlo codes. Examples are:

(i)Universal code numbers for particles and nuclei in the computer codes. The Particle Data Group proposed such a Monte Carlo particle numbering scheme, see for instance [58]. This scheme is used for the output of events by many event generators (examples are PYTHIA, JETSET and other Lund codes, HERWIG and the DPM event generators DPMJET and PHOJET), but the scheme is not suitable for the internal running of the codes, therefore each event generator uses a second (internal) particle numbering scheme. It would certainly be of advantage to standardize also these internal particle codes.

(ii)A standard COMMON block for the presentation of the Monte Carlo events was proposed by working groups for the LEP and LHC colliders. The structure of this common block has been suggested in Refs. [59,60]. This standard COMMON follows closely a scheme first used in Monte Carlo codes of the Lund group. This COMMON contains not only the final particles produced in the collisions, it also documents all the internal features of the model, for instance: original projectile and target particles, partons, chains formed out of the partons, hadronization of chains, decay of unstable particles, intranuclear cascade interactions, excited nuclei, evaporation particles and stable residual nuclei and nuclear fragments.

(iii)A similar effort has been started by the community of heavy ion experiments for the event generators for heavy ion collisions [61].

5 Conclusions

Most hadronic event generators which can be used for simulating hadronic and nuclear collisions up to the highest energies are quite similar in their construction and in the underlying theoretical concepts. At energies, where data from accelerator and collider experiments are available the models agree rather well with each other and with the most important features of the data. As soon as we compare the extrapolations of the models at higher energy we find in spite of the similarities in the underlying theoretical concepts quite often striking differences between the predictions of the models. We conclude: (i) Measurements of inclusive hadron production at the TEVATRON Collider and in the future at the LHC collider are very important to guide the models. (ii) More theoretical efforts to improve the hadronic and nuclear collision models are needed to get better extrapolations. (iii)Cosmic ray experiments should use in the high energy region simulations with more than one hadronic interaction model for interpreting their data.

6 Acknowledgments

The author thanks D.Heck for providing him with the CORSIKA code, J.Knapp for Fig. 9 and R.Engel for providing him with the SIBYLL–1.7 code and for useful discussions.

References

1. G. Ingelman and P. E. Schlein, *Phys. Lett.* B152(1985)256.
2. R. Bonino et al., *Phys. Lett.* B211(1988)239.
3. F. Abe et al., *Phys.Rev. Lett.* 80(1998)1156.
4. B. Abbott et al., *Phys. Lett.* B440(1998)189.
5. NA35 Collaboration, T. Alber et al. , *Z. Phys.* C 64(1994)195.
6. NA35 Collaboration, T. Alber et al. , *Eur. Z. Phys.* C2(1998)643.
7. J. Ranft, Baryon stopping in high energy collisions and the extrapolation of hadron production models to cosmic ray energies, Preprint *hep–ph/0002137*, 2000.
8. J. Ranft, R. Engel and S. Roesler, Baryon stopping in high energy collisions in the DPMJET–III model, presented at the same meeting by J. Ranft 2000.
9. T. Sjöstrand, *Comp. Phys. Comm.* 82(1994)74.
10. T. Sjöstrand, PYTHIA 5.7 and JETSET 7.4, physics and manual, CERN Report CERN-TH.7112/93, (revised August 1995) 1995.
11. G. Marchesini, B. Webber, G. Abbiendi, I. Knowles, M. Seymour and I. Stanco, *Computer Phys. Comm.* 67(1992)465.
12. H. Baer, F. E. Paige, S. D. Protopopescu and X. Tata, Isajet 7.48: A monte carlo event generator for pp and $\bar{p}p$ and e^+e^- reactions, Preprint BNL–HET–99/43, 1999.
13. X. N. Wang and M. Gyulassy, Hijing: A monte carlo model for multiple jet production in pp, pa, and aa collisions, *Phys. Rev.* D44(1991)3501.
14. B. Andersson, G. Gustafson and H. Pi, *Z. Phys.* C57(1993)485.

15. P. R. Sala, Fluka: status and perspectives for hadronic applications, Contribution to this meeting, 2000.
16. J. P. Wellisch, On hadronic models in geant4, Contribution to this meeting, 2000.
17. R. Engel, *Z. Phys.* C66(1995)203.
18. R. Engel and J. Ranft, *Phys. Rev.* D54(1996)4244.
19. S. Roesler, R. Engel and J. Ranft, presented at the same meeting by S. Roesler.
20. The Auger Collaboration, Pierre Auger project design report, Fermilab report 1995.
21. N. Chila et al., *Nucl.Instr.Meth.* A 311(1992)338.
22. D. J.. Bird et al., *Proc. 23 nd ICRC (Calgary)* 2(1993)38.
23. Abu-Zayyad, T. and others, *Nucl. Instrum. Meth.*A450(2000)253 .
24. Abu-Zayyad, T. and others, *Phys. Rev. Lett.* 84(2000)4276.
25. A. Capella, J. Tran Thanh Van and J. Kwiecinski, *Phys. Rev. Lett.* 58(1987)2015.
26. F. W. Bopp, D. Pertermann and J. Ranft, *Z. Phys.* C54(1992)683.
27. R. Engel, F. W. Bopp, D. Pertermann and J. Ranft, *Phys. Rev.* D46(1992)5192.
28. K. Hahn and J. Ranft, *Phys. Rev.* D41(1990)1463.
29. J. Ranft, *Phys. Rev.* D 51(1995)64.
30. J. Ranft, DPMJET–II, a dual parton model event generator for hadron–hadron, hadron–nucleus and nucleus–nucleus collisions, Proceedings of the second SARE workshop at CERN, 1995,ed. by G.R.Stevenson, CERN/TIS–RP/977–05, p. 144,, 1997.
31. J. Ranft, DPMJET version II.3 and II.4, Preprint *INFN/AE–97/45*, Gran Sasso report 1997.
32. J. Ranft, New features in DPMJET version II.5, *Siegen preprint Si–99–5, hep–ph/9911213*, 1999.
33. J. Ranft, DPMJET version II.5, sampling of hadron–hadron, hadron–nucleus and nucleus–nucleus interactions at accelerator and cosmic ray energies according to the two–component dual parton model, code manual, *Siegen preprint SI–99–6, hep–ph/9911232*, 1999.
34. G. Battistoni, C. Forti and J. Ranft, *Astroparticle Phys.* 3(1995)157.
35. S. P.. Ahlen et al., *Nucl. Instr. Meth.* A 324(1993)337.
36. J. Knapp and D. Heck, Extensive air shower simulation with corsika, *KFK 5196 B*, Karlsruhe report 1993.
37. R. S. Fletcher, T. K. Gaisser, P. Lipari and T. Stanev, *Phys. Rev.* D50(1994)5710.
38. E. Eichten et al., *Rev. Mod. Phys.* 56(1984)579.
39. R. Engel, T. K. Gaisser and T. Stanev, Air shower calculations with the new version os sibyll, Proceedings of the 25th International Cosmic Ray Conference, Utah, 1999, vol.1, p.415 1999.
40. S. C. Sciutto, Aires, a system for air shower simulations, version 2.2.0, *astro–ph/9911331* 1999.
41. A. Hillas, *J.Phys.G* 8(1982)1461;1475.
42. A. M. Hillas, *Nucl. Phys. B (Proc. Suppl.)* 52(1997)29.
43. K. Werner, *Phys. Rep.* 232(1993)87.
44. S. Ostapchenko, T. Thouw and K. Werner, *Nucl. Phys. B* 52B(1997)3.
45. H. J. Drescher, M. Hladik, S. Ostapchenko, T. Pierog and K. Werner, On the role of energy conservation in high–energy nuclear scattering, Preprint *hep–ph/0006347*, 2000.
46. N. Kalmykov et al., *Physics of Atomic Nuclei* 58(1995)1728.
47. J. Engel, T.K. Gaisser, P. Lipari and T. Stanev, *Phys. Rev.* D46(1992)5013.

48. J. Knapp, D. Heck and G. Schatz, Comparison of hadronic interaction models used in air shower simulations and their influence on shower development and observables, Preprint FZKA 5828, Karlsruhe report 1996.
49. J. Knapp and D. Heck, Extensive air shower simulation with corsika, a users guide, Karlsruhe report 1998.
50. P. Doll et al., The Karlsruhe cosmic ray project KASKADE, *KFK 4686*, Karlsruhe report 1990.
51. L. A. Anchordoqui, M. D. Dova, L. N. Epele and S. J. Sciutto, Hadronic interaction models beyond collider energies, *hep–ph/9810384* 1998.
52. R. Engel, T. K. Gaisser and T. Stanev, Extensive air showers and hadronic interaction models, Proceedings of ISMD99, International Symposium on multiparticle dynamics, Providence, R.I. 1999, ed. by I.Sarcevic and C.–I. Tan. World Scientific p.457 2000.
53. R. Engel, *Nucl. Phys. (Proc. Suppl.)* 75A(1999)62.
54. D. Kharzeev, *Phys.Lett.* B 378(1996)238.
55. A. Capella and B. Kopeliovich, *Phys. Lett.* B381(1996)325.
56. T. K. Gaisser, *Cosmic Rays and Particle Physics,*, Cambridge University Press, 1990.
57. J. Capdeveille, *J.Phys. G* 15(1989)909.
58. C. Caso et al., Review of particle properties, *European Phys. Journ.* C 3(1998)1.
59. G. Altarelli, R. Kleiss and C. Verzegnassi (Eds.), Z Physics at LEP 1, Vol. 3:Event generators and software CERN 89–08 v.3 (Sept. 1989) pp.327 1989.
60. F. Carminati, O. DiRosa, B. van Eijk, I. Zacharov, D. Hatzifotiadou, Standard interfaces between modules of event generators using dynamical common structures, Proc. Large Hadron Collider workshop, CERN 90–10 vol. III(1990) CERN 90–10 vol. III (1990) pp. 52 1990.
61. OSCAR, See details on OSCAR home page http://rhic.phys.columbia.edu/oscar/.